'Critical window variable selection: estimating the impact of air pollution on very preterm birth' Supplementary Materials

Joshua L. Warren[*,a], Wenjing Kong[a], Thomas J. Luben[b], Howard H. Chang[c]

[a]Department of Biostatistics, Yale University, New Haven, CT 06520, USA

[b]United States Environmental Protection Agency, Durham, NC 27709, USA

[c]Department of Biostatistics and Bioinformatics, Emory University, Atlanta, GA 30322, USA

S1 Model Fitting Details

We fit critical window variable selection (CWVS) using Markov chain Monte Carlo sampling techniques, including Gibbs and Metropolis (within Gibbs) sampling algorithms (Metropolis *and others*, 1953; Geman and Geman, 1984; Gelfand and Smith, 1990). All models are fit using R statistical software (R Core Team, 2017). We rely on the latent variable approach of Polson *and others* (2013) to allow for closed form full conditionals within our logistic regression framework for the included regression parameters. Specifically, we introduce

$$w_i|\boldsymbol{\beta}, \boldsymbol{\alpha} \overset{\text{ind}}{\sim} \text{Pólya-Gamma}\left(1, \mathbf{x}_i^{\mathrm{T}}\boldsymbol{\beta} + \mathbf{z}_i^{\mathrm{T}}\boldsymbol{\alpha}\right),$$

$i = 1, \ldots, n$; one latent variable for each observed Y_i binary response variable. The length m vector of exposures specific to subject i is given as $\mathbf{z}_i$ such that the t^{th} entry is $\mathbf{z}_{it} = \mathrm{z}_i\left\{c_i\left(t\right)\right\}$; and $\boldsymbol{\alpha} = \left\{\alpha\left(1\right), \ldots, \alpha\left(m\right)\right\}^{\mathrm{T}}$. Using these latent variables, we derive the full conditional densities needed for posterior sampling.

From Polson *and others* (2013), the full conditional distributions of the w_i latent variables are given as

$$w_i|\boldsymbol{Y}, \Theta_{-w_i} \overset{\text{ind}}{\sim} \text{Pólya-Gamma}\left(1, \mathbf{x}_i^{\mathrm{T}}\boldsymbol{\beta} + \mathbf{z}_i^{\mathrm{T}}\boldsymbol{\alpha}\right),\ i = 1, \ldots, n$$

where $\boldsymbol{Y} = \left(Y_1, \ldots, Y_n\right)^{\mathrm{T}}$ and Θ_{-w_i} represents all latent variables and model parameters after removing w_i. Note that the full conditional and prior distributions are identical for these parameters given the lack of dependence between w_i and Y_i (unlike the latent parameters in probit regression). We sample from this distribution using the `BayesLogit` package in R (Polson *and others*, 2013) and note that it does not depend on the observed data, $\boldsymbol{Y}$.

The vector of regression parameters associated with the covariates and confounders also has a closed form full conditional density such that $\boldsymbol{\beta}|\boldsymbol{Y}, \Theta_{-\boldsymbol{\beta}} \sim \text{MVN}\left(\boldsymbol{\mu}_{\boldsymbol{\beta}}, \Sigma_{\boldsymbol{\beta}}\right)$ with

$$\Sigma_\beta = \left(\mathrm{X}^{\mathrm{T}}\Omega\mathrm{X} + \frac{1}{\sigma^2_{\boldsymbol{\beta}}}I_p\right)^{-1},\ \mu_\beta = \Sigma_\beta\left\{\mathrm{X}^{\mathrm{T}}\Omega\left(\boldsymbol{\lambda} - \mathrm{Z}\boldsymbol{\alpha}\right)\right\}$$

where $\Omega_{ii} = w_i$ for $i = 1, \ldots, n$ and $\Omega_{ij} = 0$ for $i \neq j$; $\boldsymbol{\lambda} = \{(Y_1 - 0.50)/w_1, \ldots, (Y_n - 0.50)/w_n\}^{\mathrm{T}}$; X is an n by p matrix with i^{th} row equal to $\mathbf{x}_i^{\mathrm{T}}$; and Z is an n by s matrix with i^{th} row equal to $\mathbf{z}_i^{\mathrm{T}}$.

The variable selection parameters have independent Bernoulli full conditional distributions such that $\gamma(t)|\boldsymbol{Y}, \Theta_{-\gamma(t)} \overset{\text{ind}}{\sim} \text{Bernoulli}(\kappa(t))$ where $\kappa(t) =$

$$\frac{\exp\left\{-\frac{1}{2}\left(\boldsymbol{\lambda} - \mathrm{X}\boldsymbol{\beta} - \mathrm{Z}\boldsymbol{\alpha}_{\{\gamma(t)=1\}}\right)^{\mathrm{T}}\Omega\left(\boldsymbol{\lambda} - \mathrm{X}\boldsymbol{\beta} - \mathrm{Z}\boldsymbol{\alpha}_{\{\gamma(t)=1\}}\right)\right\}\pi(t)}{\sum_{j=0}^{1}\exp\left\{-\frac{1}{2}\left(\boldsymbol{\lambda} - \mathrm{X}\boldsymbol{\beta} - \mathrm{Z}\boldsymbol{\alpha}_{\{\gamma(t)=j\}}\right)^{\mathrm{T}}\Omega\left(\boldsymbol{\lambda} - \mathrm{X}\boldsymbol{\beta} - \mathrm{Z}\boldsymbol{\alpha}_{\{\gamma(t)=j\}}\right)\right\}\pi(t)^{I(j=1)}\{1-\pi(t)\}^{I(j=0)}}$$

for $t = 1, \ldots, m$ where $\boldsymbol{\alpha}_{\{\gamma(t)=j\}}$ is the vector of $\alpha(t)$ parameters defined by $\gamma(t) = j$ and $I(.)$ is the indicator function taking a value of one if the input statement is true and zero otherwise.

We introduce independent, normally distributed latent variables which define the underlying probability of a one or zero for $\gamma(t)$ such that $\gamma^*(t)|\eta(t) \overset{\text{ind}}{\sim} \mathrm{N}\{\eta(t), 1\}$, $t = 1, \ldots, m$ and $\pi(t) = \mathrm{P}\{\gamma^*(t) > 0\}$. The full conditional density of one of these latent parameters is given as $\gamma^*(t)|\boldsymbol{Y}, \Theta_{-\gamma^*(t)} \overset{\text{ind}}{\sim} \text{Truncated Normal}\{\eta(t), 1\}$, $t = 1, \ldots, m$ where the truncation is ≤ 0 if $\gamma(t) = 0$ and is > 0 if $\gamma(t) = 1$. Introduction of these latent parameters allows us to obtain a closed-form full conditional for $\boldsymbol{\delta}_2$ such that $\boldsymbol{\delta}_2|\boldsymbol{Y}, \Theta_{-\boldsymbol{\delta}_2} \sim \text{MVN}\left(\boldsymbol{\mu}_{\boldsymbol{\delta}_2}, \Sigma_{\boldsymbol{\delta}_2}\right)$ where

$$\Sigma_{\boldsymbol{\delta}_2} = \left\{A_{22}^2 I_m + \Sigma(\phi_2)^{-1}\right\}^{-1}, \ \mu_{\boldsymbol{\delta}_2} = \Sigma_{\boldsymbol{\delta}_2}\left\{A_{22}(\boldsymbol{\gamma}^* - A_{21}\boldsymbol{\delta}_1)\right\}$$

where $\boldsymbol{\gamma}^* = \{\gamma^*(1), \ldots, \gamma^*(m)\}^{\mathrm{T}}$. Similarly, $\boldsymbol{\delta}_1$ has a $\text{MVN}\left(\boldsymbol{\mu}_{\boldsymbol{\delta}_1}, \Sigma_{\boldsymbol{\delta}_1}\right)$ full conditional distribution with

$$\Sigma_{\boldsymbol{\delta}_1} = \left\{A_{11}^2 \mathrm{Z}^{*\mathrm{T}}\Omega\mathrm{Z}^* + A_{21}^2 I_m + \Sigma(\phi_1)^{-1}\right\}^{-1},$$

$$\mu_{\boldsymbol{\delta}_1} = \Sigma_{\boldsymbol{\delta}_1}\left\{A_{11}\mathrm{Z}^{*\mathrm{T}}\Omega(\boldsymbol{\lambda} - \mathrm{X}\boldsymbol{\beta}) + A_{21}(\boldsymbol{\gamma}^* - A_{22}\boldsymbol{\delta}_2)\right\}$$

where Z^* is an n by m matrix with $(i,t)^{th}$ entry $\mathrm{Z}_{it}^* = \mathrm{z}_i\{c_i(t)\}\gamma(t)$.

Metropolis sampling is required for the entries of the A matrix. For A_{21}, the full conditional density is proportional to

$$\exp\left\{-\frac{1}{2}(\boldsymbol{\gamma}^* - A_{21}\boldsymbol{\delta}_1 - A_{22}\boldsymbol{\delta}_2)^{\mathrm{T}}(\boldsymbol{\gamma}^* - A_{21}\boldsymbol{\delta}_1 - A_{22}\boldsymbol{\delta}_2) - \frac{1}{2\sigma_A^2}A_{21}^2\right\}.$$

The full conditional distribution for $\ln(A_{22})$ has the same form with $-\frac{1}{2\sigma_A^2}A_{21}^2$ replaced by $-\frac{1}{2\sigma_A^2}\ln(A_{22})^2$. For $\ln(A_{11})$, the full conditional density if proportional to

$$\exp\left\{-\frac{1}{2}\left(\boldsymbol{\lambda}-\mathrm{X}\boldsymbol{\beta}-A_{11}\mathrm{Z}^*\boldsymbol{\delta}_1\right)^{\mathrm{T}}\Omega\left(\boldsymbol{\lambda}-\mathrm{X}\boldsymbol{\beta}-A_{11}\mathrm{Z}^*\boldsymbol{\delta}_1\right)-\frac{1}{2\sigma_A^2}\ln(A_{11})^2\right\}.$$

Finally, the two parameters that control the smoothness of the processes over time also require a Metropolis step with their full conditional densities proportional to

$$\frac{1}{|\Sigma(\phi_j)|^{1/2}}\exp\left\{-\frac{1}{2}\boldsymbol{\delta}_j^{\mathrm{T}}\Sigma(\phi_j)^{-1}\boldsymbol{\delta}_j\right\}\exp\left\{\alpha_\phi\psi_j-\beta_\phi\exp\{\psi_j\}\right\}$$

for $j=0,1$. We transform each of these parameters to have support on the real line (working with the induced prior distribution) in order to improve properties of the posterior sampling such that $\psi_j=\ln(\phi_j)\in\mathbb{R}$.

S2 Additional Simulation Studies

We design additional simulation studies to compare the performance of the Gaussian process (GP) model and the linear model of coregionalization version of CWVS when the true risk parameters, $\alpha(t)$, are smoothly varying across pregnancy (i.e., no parameters are exactly zero). Results from GP and CWVS will be similar when $\gamma(t) = 1$ for most or all t. However, this condition does not depend on the level of smoothness in $\alpha(t)$. Instead, estimated $\gamma(t)$ will equal one for most or all t if the individual risk parameters are large enough in magnitude. Therefore, we hypothesize that whenever the risk parameters are large and there is sufficient data to detect them, leading to estimated $\gamma(t) = 1$ for most or all t, that GP and CWVS will perform similarly, regardless of the smoothness pattern of $\alpha(t)$. We also hypothesize that smoothness in $\alpha(t)$ alone is not enough to result in nearly identical behavior between GP and CWVS. We design our simulation studies to investigate these hypotheses.

These simulation studies closely resemble those from Section 4 of the main text where $\alpha(t)$ are now assumed to vary smoothly across pregnancy times (i.e., no actual zeros). In order to create a realistic pattern of $\alpha(t)$ smoothness, we use the estimated risk parameters from GP in the ozone data application from Section 5 of the main text as a starting point (see the upper left panel of Figure 1). We then define three different versions of the true $\alpha(t)$ parameters. First, we use the GP estimates directly to reflect a realistically smooth set of risk parameters (i.e., Smooth). Next, we multiply the GP estimates by 40 in order to create smooth but easily detected risk parameters at each pregnancy week (i.e., Inflated Smooth). Lastly, we multiply the GP estimates by 40 and randomly mix-up the temporal order of the $\alpha(t)$ parameters in order to create easily detected but non-smooth risk parameters (i.e., Inflated Non-Smooth). We simulate 50 datasets from each setting, analyze them using GP and CWVS, and compare the average mean squared error (MSE), average empirical coverage of the 95% credible intervals, and critical window identification patterns of each method. The first two summary statistics are described in Section 4.3.

To determine the level of agreement between the two methods with respect to critical window identification, we compute $\frac{1}{(50)(27)} \sum_{j=1}^{50} \sum_{t=1}^{27} I\left\{\mathrm{CW}_j^{GP}(t) = \mathrm{CW}_j^{CWVS}(t)\right\}$ where $\mathrm{CW}_j^{GP}(t)$ is an indicator that is equal to one if GP identified time period t as a critical window for simulated dataset j and is equal to zero otherwise. A similar definition is given for $\mathrm{CW}_j^{CWVS}(t)$. Values of this statistic near one indicate close agreement between the two methods.

The results in Table S1 suggest that GP is more efficient in estimating the risk parameters with respect to average MSE in the Smooth setting. This is not unexpected since CWVS is likely treating some of the parameters with true values near zero as unimportant and therefore, removing them from the model, while GP is separately estimating each parameter. However, both methods report similar average empirical coverage and often agree with respect to critical window identification. In both of the inflated risk parameter settings (Inflated Smooth, Inflated Non-Smooth), GP and CWVS perform nearly identically in all monitored categories. In summary, regardless of whether the true pattern of risk parameters is smooth or not, GP and CWVS will return nearly identical results if nearly all of the risk parameters are suitably large enough in magnitude to result in high statistical power for detection.

Table S1: Average mean squared error (MSE), average empirical coverage, and level of critical window identification agreement between GP and CWVS simulation study results across all simulation settings. Standard errors are given in parentheses.

Metric	Method	Smooth	Inflated Smooth	Inflated Non-Smooth
MSE*1000	GP	0.28 (0.06)	26.76 (5.19)	25.37 (4.77)
	CWVS LMC	0.47 (0.11)	28.14 (5.53)	26.50 (5.13)
Coverage	GP	0.99 (0.01)	0.95 (0.03)	0.96 (0.03)
	CWVS LMC	0.99 (0.01)	0.94 (0.03)	0.95 (0.03)
Agreement		0.91 (0.01)	0.99 (0.00)	0.99 (0.00)

S3 Additional Tables and Figures

Table S2: Background information for the study population in North Carolina, 2005-2008.

Characteristic	Cases ($<$ 32 Weeks)	Controls ($\geq$ 32 Weeks)
Total	3,672	14,688
Smoked (Proportion Yes)	0.16	0.11
Diabetes (Proportion Yes)	0.04	0.03
Parity (No Previous Births)	0.46	0.41
Age Category:		
[15-25)	0.42	0.38
[25-30)	0.25	0.27
[30-35)	0.19	0.22
[35-50]	0.14	0.13
Race/Ethnicity:		
White Non-Hispanic	0.44	0.56
Black Non-Hispanic	0.41	0.23
Hispanic	0.12	0.17
Other	0.04	0.04
Education:		
$<$ High School	0.25	0.22
High School	0.33	0.29
$>$ High School	0.42	0.49
Sex (Female)	0.47	0.49
Marriage Status (Unmarried)	0.55	0.40
Prenatal Care Initiation (First Trimester)	0.84	0.83

Table S3: Simulation study results to determine the most appropriate critical time period definition. The proportion of times that each definition correctly identifies the true set of critical time periods, without penalty for misclassifying non-important time periods, is presented across all simulation settings. Standard errors are presented in parentheses following the estimate. Median probability: $P\{\gamma(t) = 1|\boldsymbol{Y}\} \geq 0.50$; Credible interval: 95% credible interval of $\alpha(t)|\gamma(t) = 1$ excludes zero.

Method	E1	M1	E4	M4	E7	M7
Median Probability						
SSVS	1.00 (0.00)	1.00 (0.00)	0.32 (0.07)	0.14 (0.05)	0.00 (0.00)	0.00 (0.00)
CWVS Sep.	1.00 (0.00)	1.00 (0.00)	0.80 (0.06)	0.68 (0.07)	0.28 (0.06)	0.10 (0.04)
CWVS LMC	1.00 (0.00)	1.00 (0.00)	0.98 (0.02)	0.98 (0.02)	0.90 (0.04)	0.86 (0.05)
Credible Interval						
SSVS	1.00 (0.00)	1.00 (0.00)	0.68 (0.07)	0.66 (0.07)	0.02 (0.02)	0.00 (0.00)
CWVS Sep.	1.00 (0.00)	1.00 (0.00)	0.74 (0.06)	0.86 (0.05)	0.08 (0.04)	0.14 (0.05)
CWVS LMC	1.00 (0.00)	1.00 (0.00)	0.92 (0.04)	0.94 (0.03)	0.54 (0.07)	0.26 (0.06)
Median Probability & Credible Interval						
SSVS	1.00 (0.00)	1.00 (0.00)	0.32 (0.07)	0.14 (0.05)	0.00 (0.00)	0.00 (0.00)
CWVS Sep.	1.00 (0.00)	1.00 (0.00)	0.74 (0.06)	0.68 (0.07)	0.08 (0.04)	0.04 (0.03)
CWVS LMC	1.00 (0.00)	1.00 (0.00)	0.92 (0.04)	0.94 (0.03)	0.54 (0.07)	0.26 (0.06)
GP	1.00 (0.00)	1.00 (0.00)	0.96 (0.03)	0.96 (0.03)	0.42 (0.07)	0.24 (0.06)

Table S4: Standard errors corresponding to the estimates presented in Table 2 of the main text. Median probability: $P\{\gamma(t) = 1|\boldsymbol{Y}\} \geq 0.50$; Credible interval: 95% credible interval of $\alpha(t)|\gamma(t) = 1$ excludes zero.

Method	E1	M1	E4	M4	E7	M7
Median Probability						
SSVS	0.02	0.00	0.06	0.05	0.00	0.00
CWVS Sep.	0.03	0.02	0.07	0.07	0.04	0.00
CWVS LMC	0.04	0.03	0.07	0.05	0.06	0.02
Credible Interval						
SSVS	0.07	0.06	0.07	0.06	0.00	0.00
CWVS Sep.	0.07	0.07	0.07	0.07	0.03	0.03
CWVS LMC	0.07	0.07	0.06	0.07	0.07	0.05
Median Probability & Credible Interval						
SSVS	0.02	0.00	0.06	0.05	0.00	0.00
CWVS Sep.	0.03	0.02	0.07	0.07	0.03	0.02
CWVS LMC	0.04	0.03	0.06	0.07	0.07	0.05
GP	0.07	0.07	0.07	0.07	0.07	0.06

Table S5: Standard errors corresponding to the estimates presented in Table 3 of the main text.

Metric	Method	E1	M1	E4	M4	E7	M7
Critical Weeks (B_1)							
MSE*1000	GP	1.70	2.58	0.13	0.22	0.09	0.09
	SSVS	0.32	0.22	0.43	0.39	0.27	0.20
	CWVS Sep.	0.34	0.29	0.33	0.29	0.22	0.15
	CWVS LMC	0.39	0.68	0.17	0.19	0.12	0.08
Coverage	GP	0.07	0.07	0.02	0.03	0.01	0.01
	SSVS	0.04	0.00	0.02	0.02	0.01	0.01
	CWVS Sep.	0.04	0.00	0.02	0.01	0.01	0.01
	CWVS LMC	0.05	0.02	0.01	0.01	0.01	0.01
Bordering Critical Weeks (B_2)							
MSE*1000	GP	1.33	0.47	0.29	0.17	0.15	0.12
	SSVS	0.56	0.26	0.69	0.51	0.68	0.65
	CWVS Sep.	0.70	0.35	0.57	0.33	0.30	0.30
	CWVS LMC	0.70	0.34	0.31	0.19	0.16	0.15
Coverage	GP	0.06	0.02	0.06	0.04	0.05	0.03
	SSVS	0.03	0.02	0.03	0.03	0.03	0.03
	CWVS Sep.	0.04	0.02	0.03	0.02	0.04	0.03
	CWVS LMC	0.05	0.02	0.04	0.03	0.04	0.03
Non-Critical, Non-Bordering Critical Weeks (B_3)							
MSE*1000	GP	0.13	0.12	0.06	0.05	0.08	0.06
	SSVS	0.11	0.16	0.16	0.14	0.20	0.22
	CWVS Sep.	0.12	0.15	0.10	0.08	0.10	0.09
	CWVS LMC	0.10	0.14	0.07	0.04	0.08	0.06
Coverage	GP	0.00	0.01	0.00	0.00	0.00	0.00
	SSVS	0.00	0.01	0.01	0.01	0.01	0.01
	CWVS Sep.	0.00	0.01	0.00	0.00	0.00	0.01
	CWVS LMC	0.01	0.01	0.00	0.00	0.00	0.00

Table S6: Geweke diagnostic results from the very preterm birth analysis in North Carolina, 2005-2008. The number of tests correspond to the number of unique parameters in each model. The number of rejections is based on the number of calculated Geweke test statistics that are larger than the $\alpha = 0.05$ critical values (two-sided) after Bonferroni adjustment for multiple testing.

Method	Mean	(Min., Max.)	# of Tests	# of Rejections
Ozone Results				
GP	-0.04	(-1.99, 2.56)	61	0
SSVS	-0.04	(-2.63, 1.97)	87	0
CWVS Sep.	-0.83	(-3.12, 2.96)	117	0
CWVS LMC	0.12	(-3.00, 3.07)	118	0
$PM_{2.5}$ Results				
GP	-0.35	(-2.72, 2.17)	61	0
SSVS	-0.10	(-2.28, 3.88)	87	1
CWVS Sep.	-0.23	(-2.12, 2.45)	117	0
CWVS LMC	0.37	(-2.83, 3.40)	118	0

Table S7: Main covariate results from the very preterm birth and ozone (8 hour maximum) exposure analysis in North Carolina, 2005-2008. Model also adjusted for temporal trends, seasonality, and spatial location. Posterior inference on the odds ratio scale is presented.

			Quantiles	
Parameter	Mean	SD	0.025	0.975
Smoked During Pregnancy:				
Yes vs. No	1.56	0.09	1.39	1.75
Diabetes Status:				
Yes vs. No	1.14	0.12	0.92	1.40
Parity:				
>0 vs. 0	0.75	0.03	0.69	0.81
Age (Years):				
[25, 30) vs. [15,25)	1.15	0.06	1.04	1.28
[30, 35) vs. [15,25)	1.33	0.08	1.18	1.49
[35,50] vs. [15,25)	1.72	0.12	1.50	1.95
Education:				
High school vs. < high school	0.94	0.05	0.85	1.05
> High school vs. < high school	0.80	0.05	0.71	0.89
Race/Ethnicity:				
Black, Non-Hispanic vs. White, Non-Hispanic	2.17	0.10	1.97	2.38
Hispanic vs. White, Non-Hispanic	0.90	0.06	0.78	1.02
Other vs. White, Non-Hispanic	1.10	0.11	0.90	1.34
Sex of Child:				
Female vs. Male	0.89	0.03	0.82	0.96
Martial Status:				
Unmarried vs. Married	1.49	0.07	1.36	1.64
Trimester when Prenatal Care Began:				
Second or Third vs. First	0.78	0.04	0.70	0.86

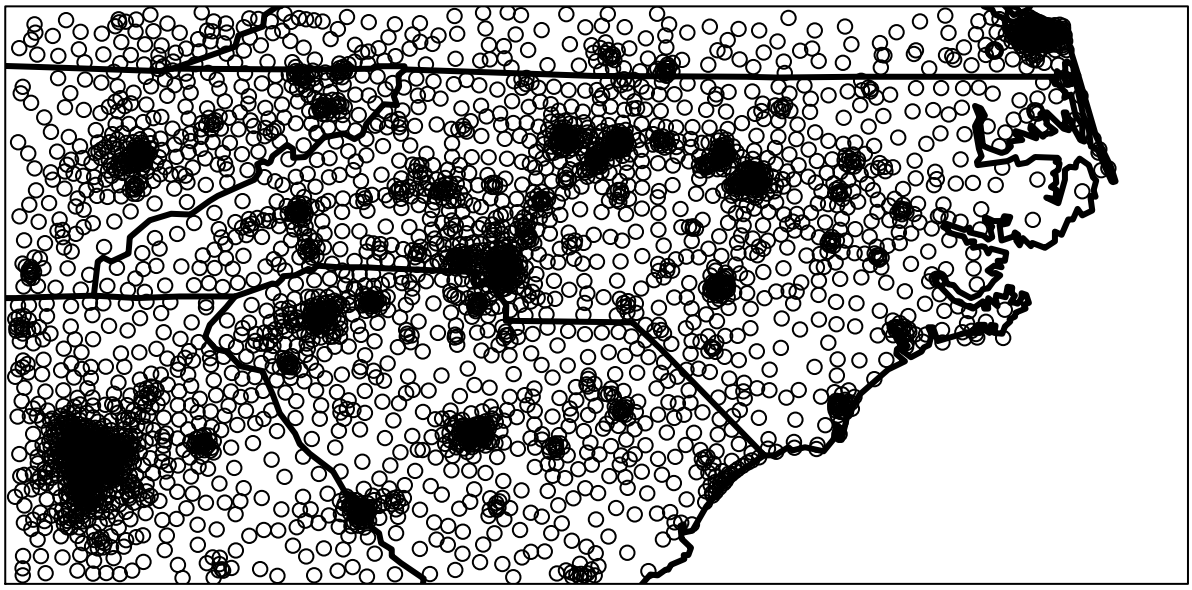

Figure S1: Year 2000 Census tract centroids where the Environmental Protection Agency fused downscaler estimates for ozone (8 hour maximum) and particulate matter less than 2.5 micrometers in aerodynamic diameter (24 hour average) are available daily.

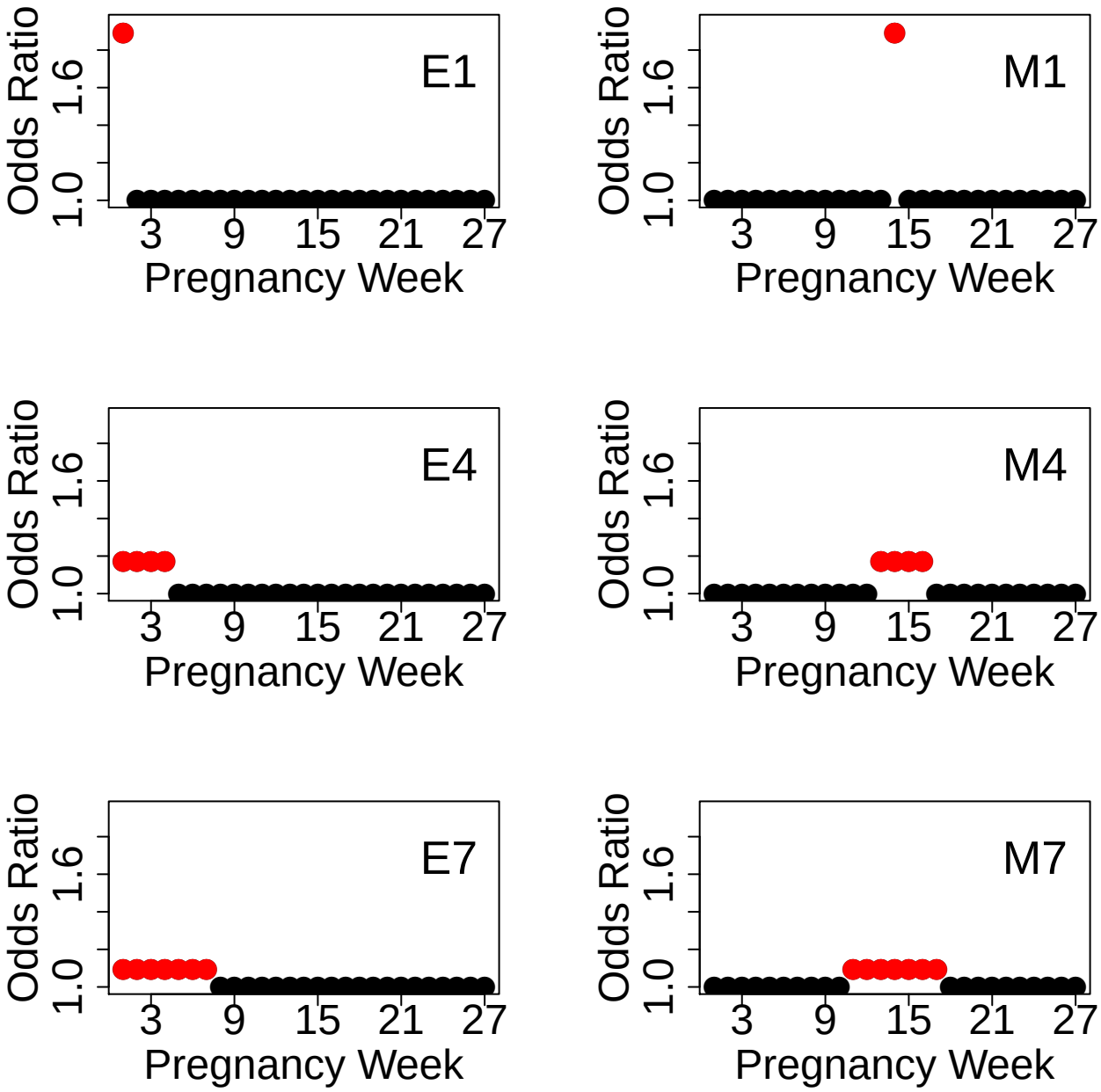

Figure S2: Simulation study data generating settings for $\alpha(t)$.

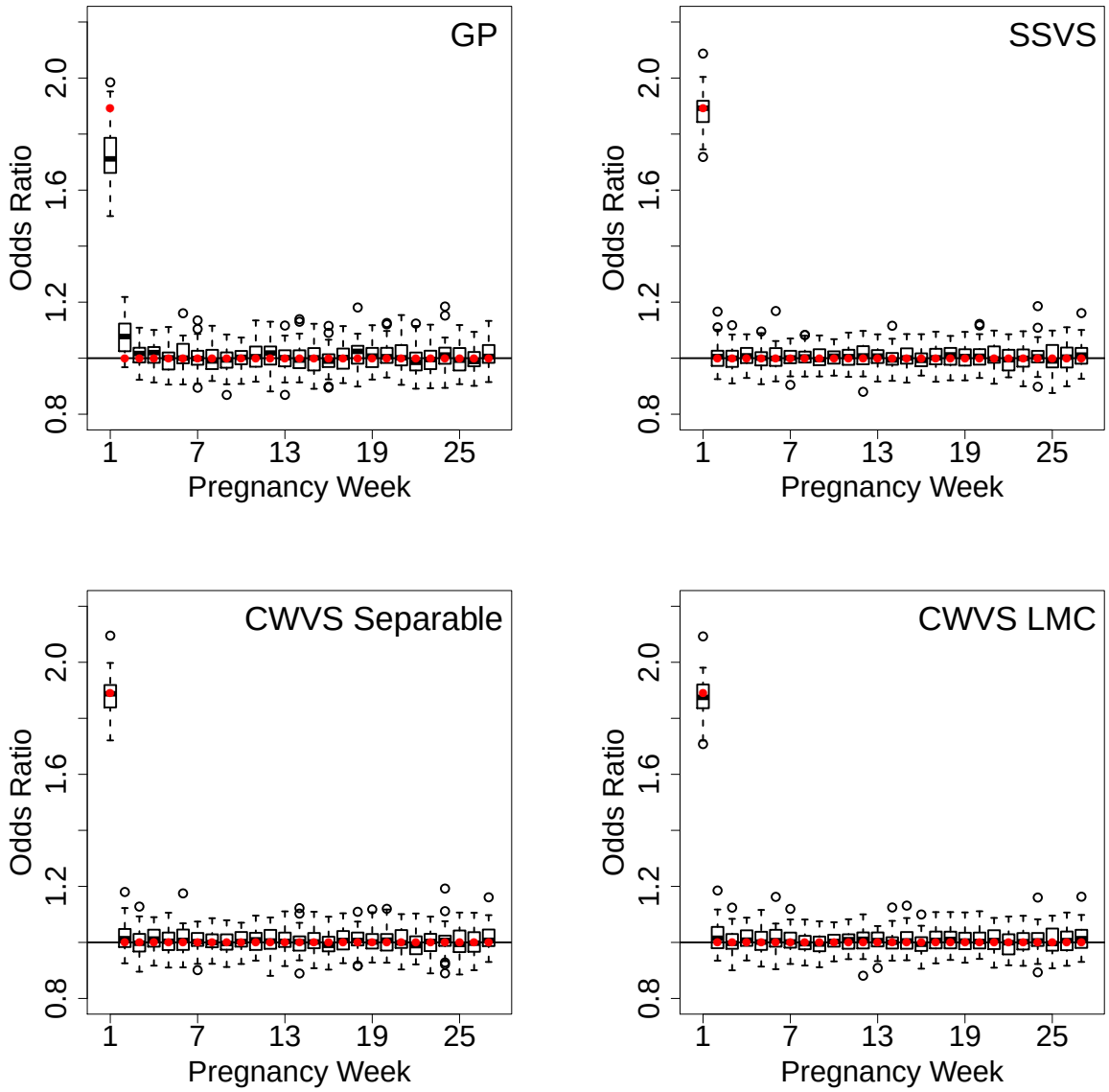

Figure S3: Simulation study results for Setting E1 (estimate behavior). Boxplots of the 50 posterior means of $\exp\{\alpha(t)\,|\gamma(t)=1\}$ (just $\exp\{\alpha(t)\}$ for GP) are presented in black. Red dots indicate the true risk parameters. All values presented on the odds ratio scale.

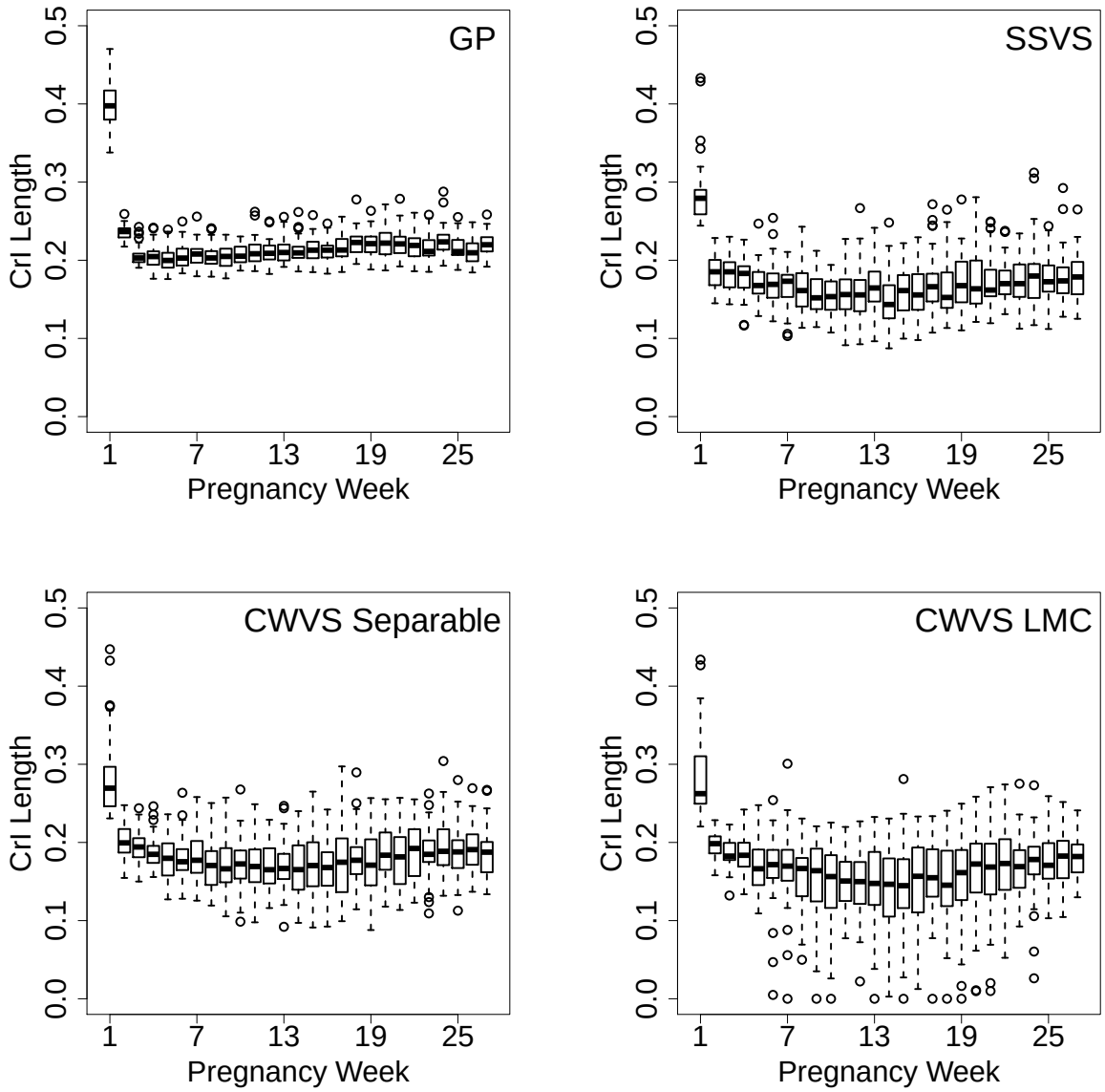

Figure S4: Simulation study results for Setting E1 (uncertainty behavior). Boxplots of the 50 quantile-based 95% credible interval lengths for $\exp\{\alpha(t)\,|\gamma(t)=1\}$ (just $\exp\{\alpha(t)\}$ for GP) are presented.

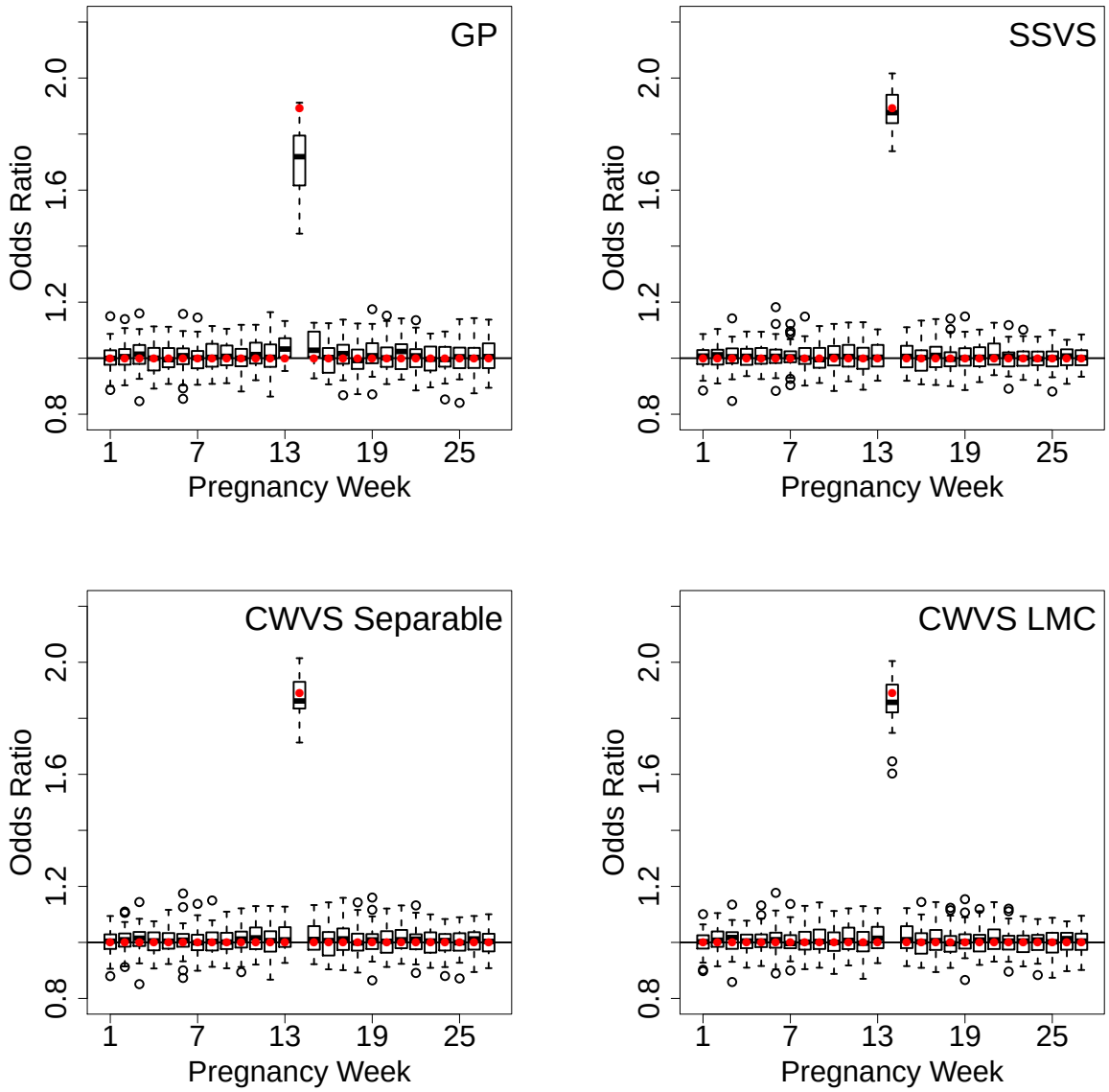

Figure S5: Simulation study results for Setting M1 (mean behavior). Boxplots of the 50 posterior means of $\exp\{\alpha(t)|\gamma(t)=1\}$ (just $\exp\{\alpha(t)\}$ for GP) are presented in black. Red dots indicate the true risk parameters. All values presented on the odds ratio scale.

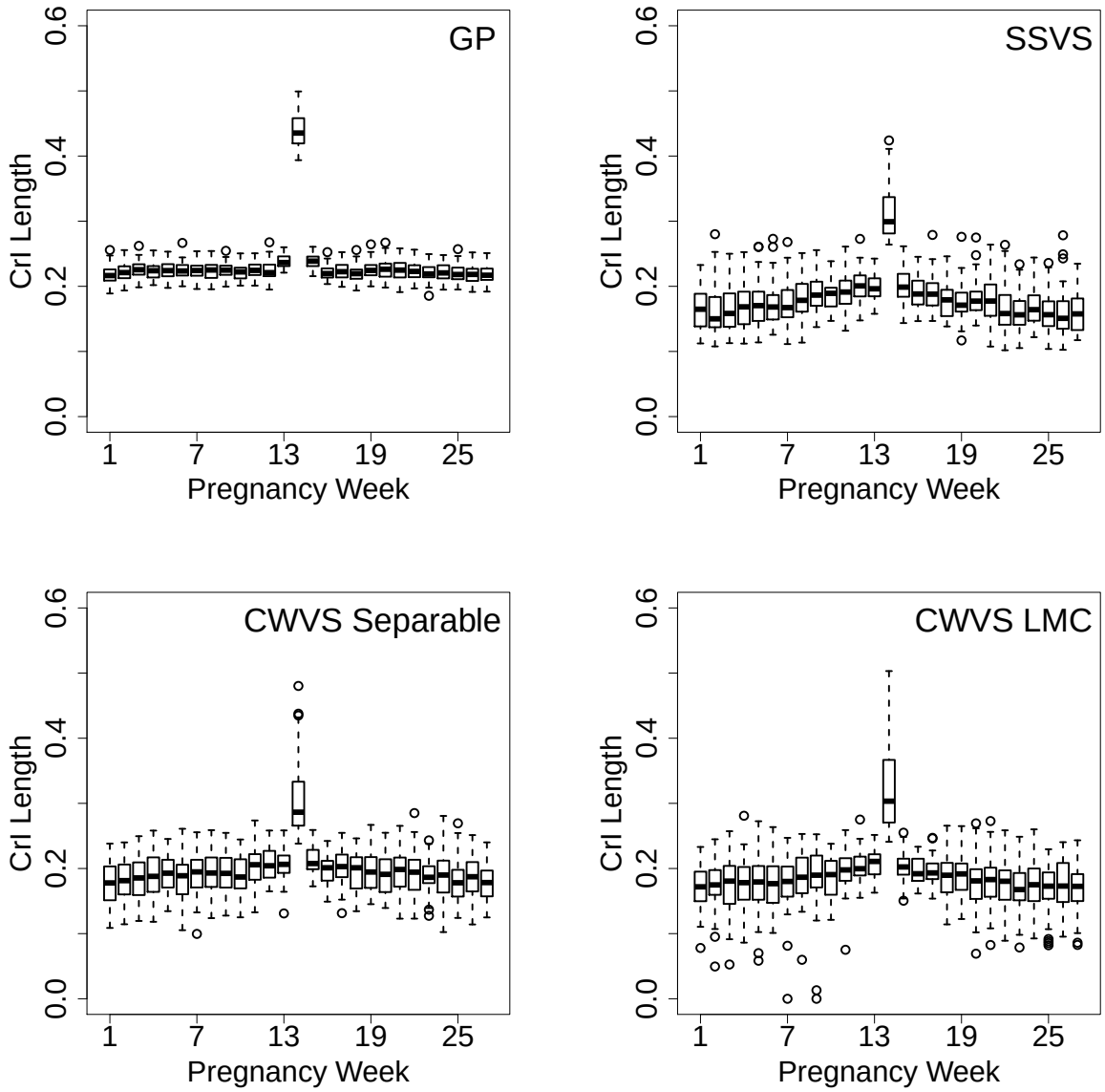

Figure S6: Simulation study results for Setting M1 (uncertainty behavior). Boxplots of the 50 quantile-based 95% credible interval lengths for $\exp\{\alpha(t)\,|\gamma(t)=1\}$ (just $\exp\{\alpha(t)\}$ for GP) are presented.

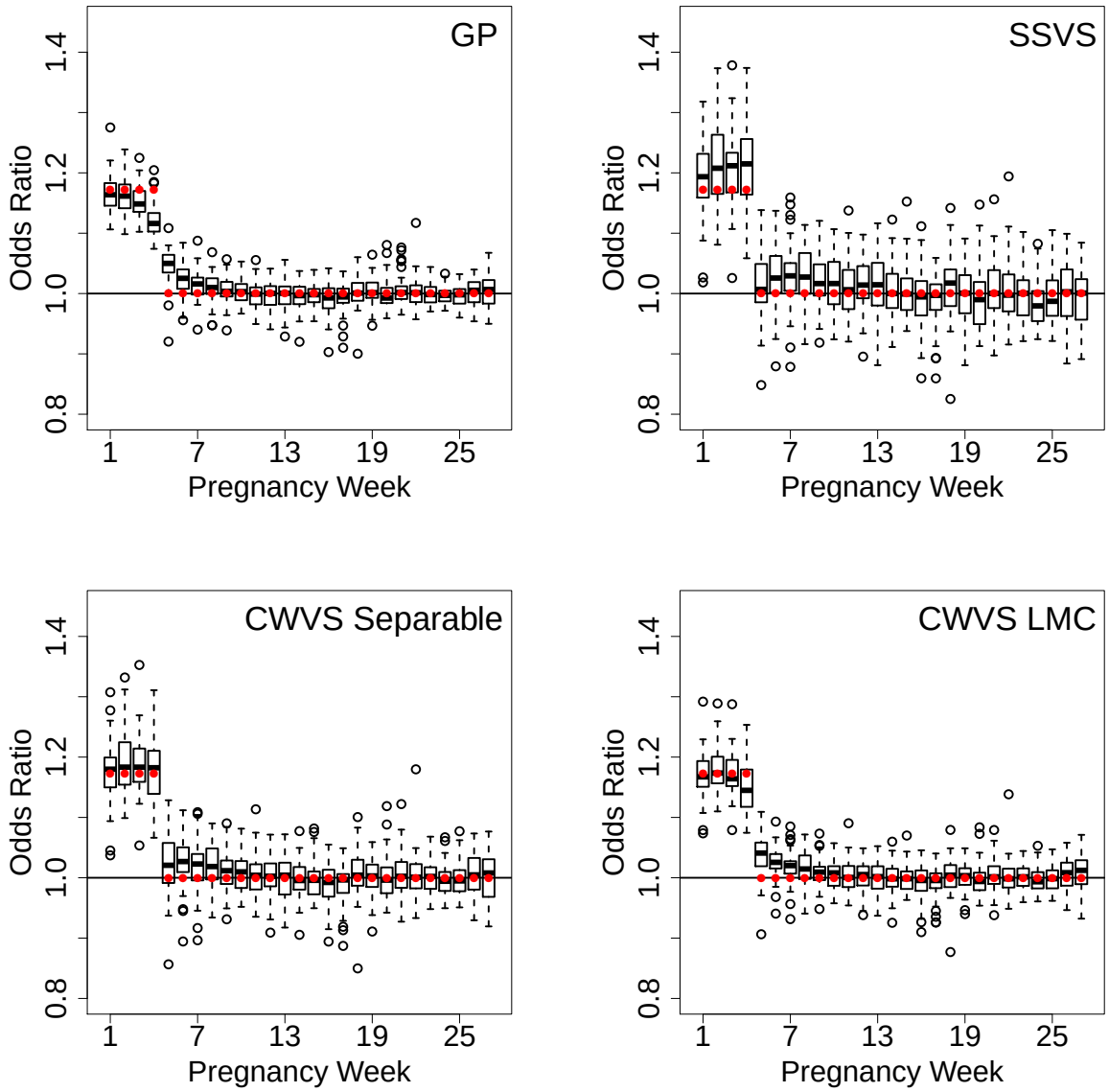

Figure S7: Simulation study results for Setting E4 (mean behavior). Boxplots of the 50 posterior means of $\exp\{\alpha(t)|\gamma(t)=1\}$ (just $\exp\{\alpha(t)\}$ for GP) are presented in black. Red dots indicate the true risk parameters. All values presented on the odds ratio scale.

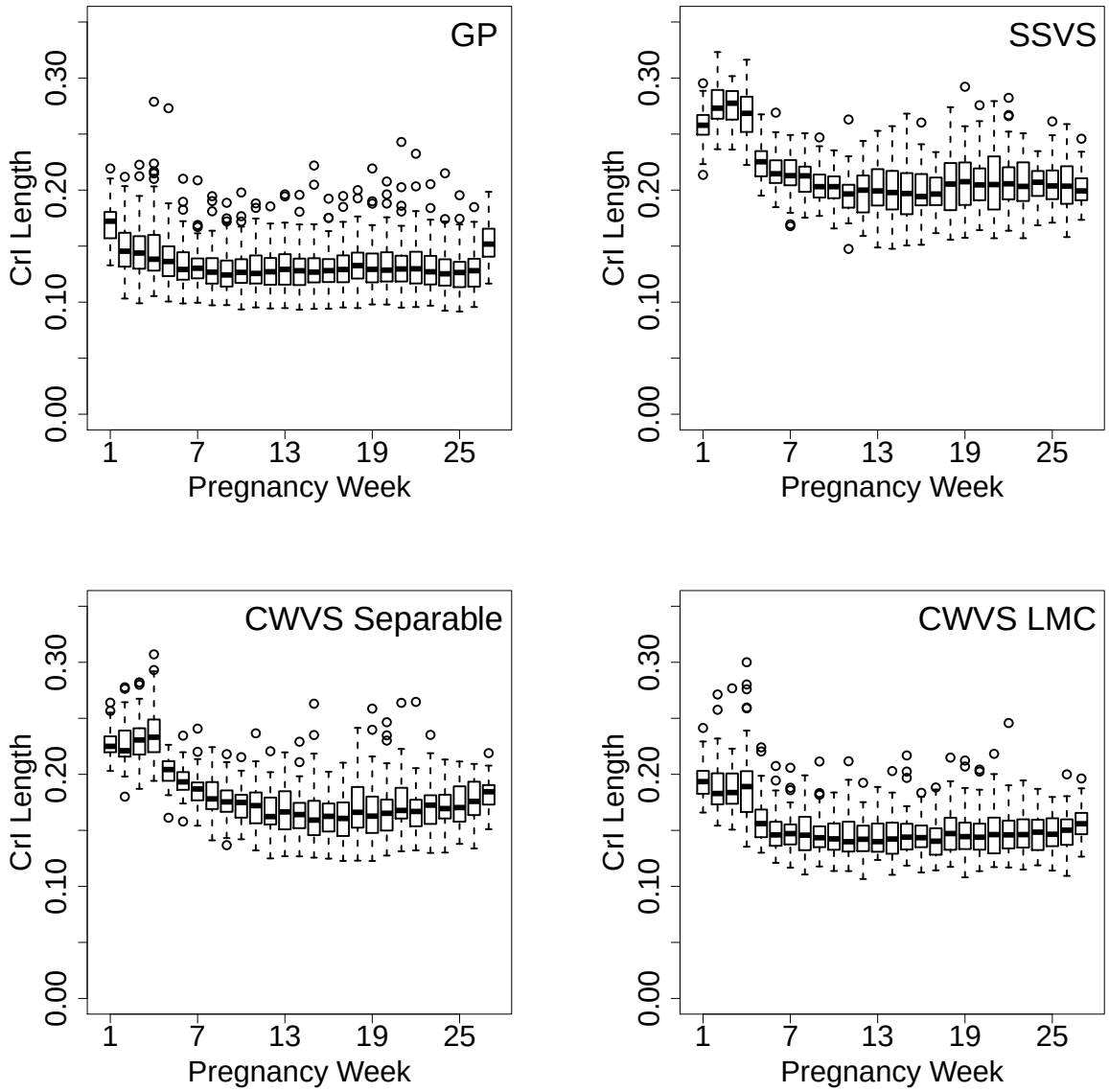

Figure S8: Simulation study results for Setting E4 (uncertainty behavior). Boxplots of the 50 quantile-based 95% credible interval lengths for $\exp\{\alpha(t)\,|\,\gamma(t)=1\}$ (just $\exp\{\alpha(t)\}$ for GP) are presented.

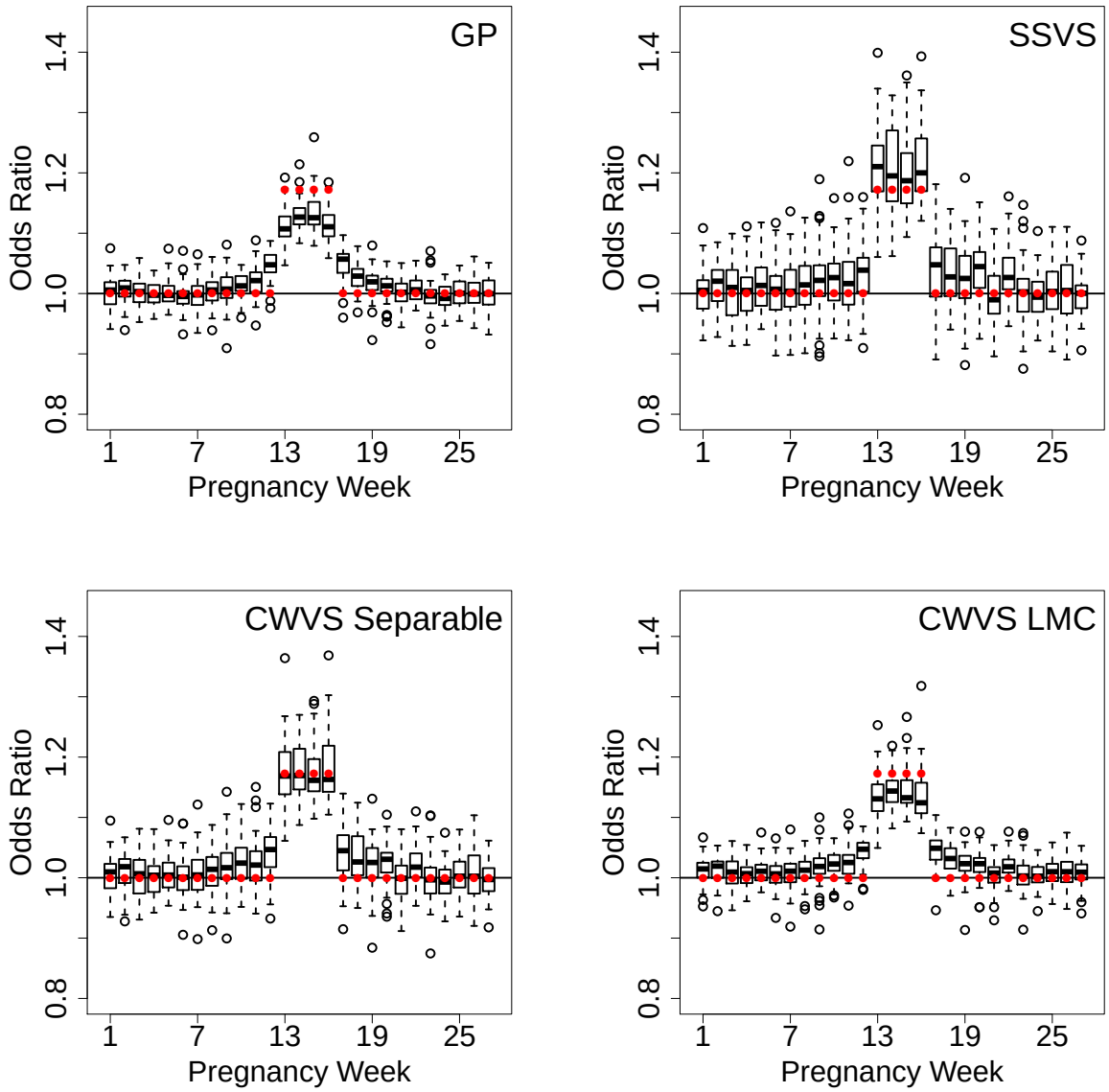

Figure S9: Simulation study results for Setting M4 (mean behavior). Boxplots of the 50 posterior means of $\exp\{\alpha(t)\,|\gamma(t)=1\}$ (just $\exp\{\alpha(t)\}$ for GP) are presented in black. Red dots indicate the true risk parameters. All values presented on the odds ratio scale.

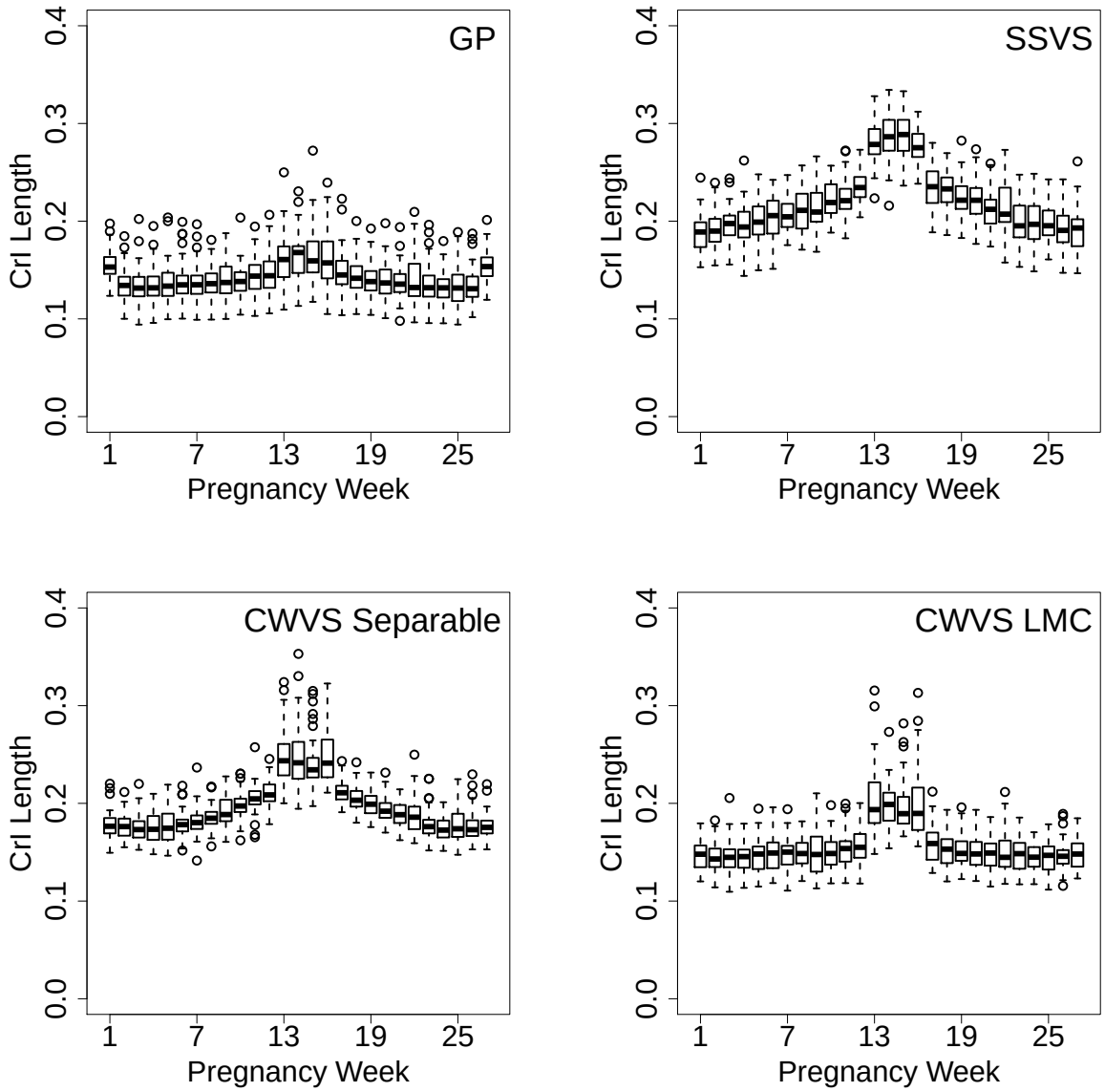

Figure S10: Simulation study results for Setting M4 (uncertainty behavior). Boxplots of the 50 quantile-based 95% credible interval lengths for $\exp\{\alpha(t)\,|\gamma(t)=1\}$ (just $\exp\{\alpha(t)\}$ for GP) are presented.

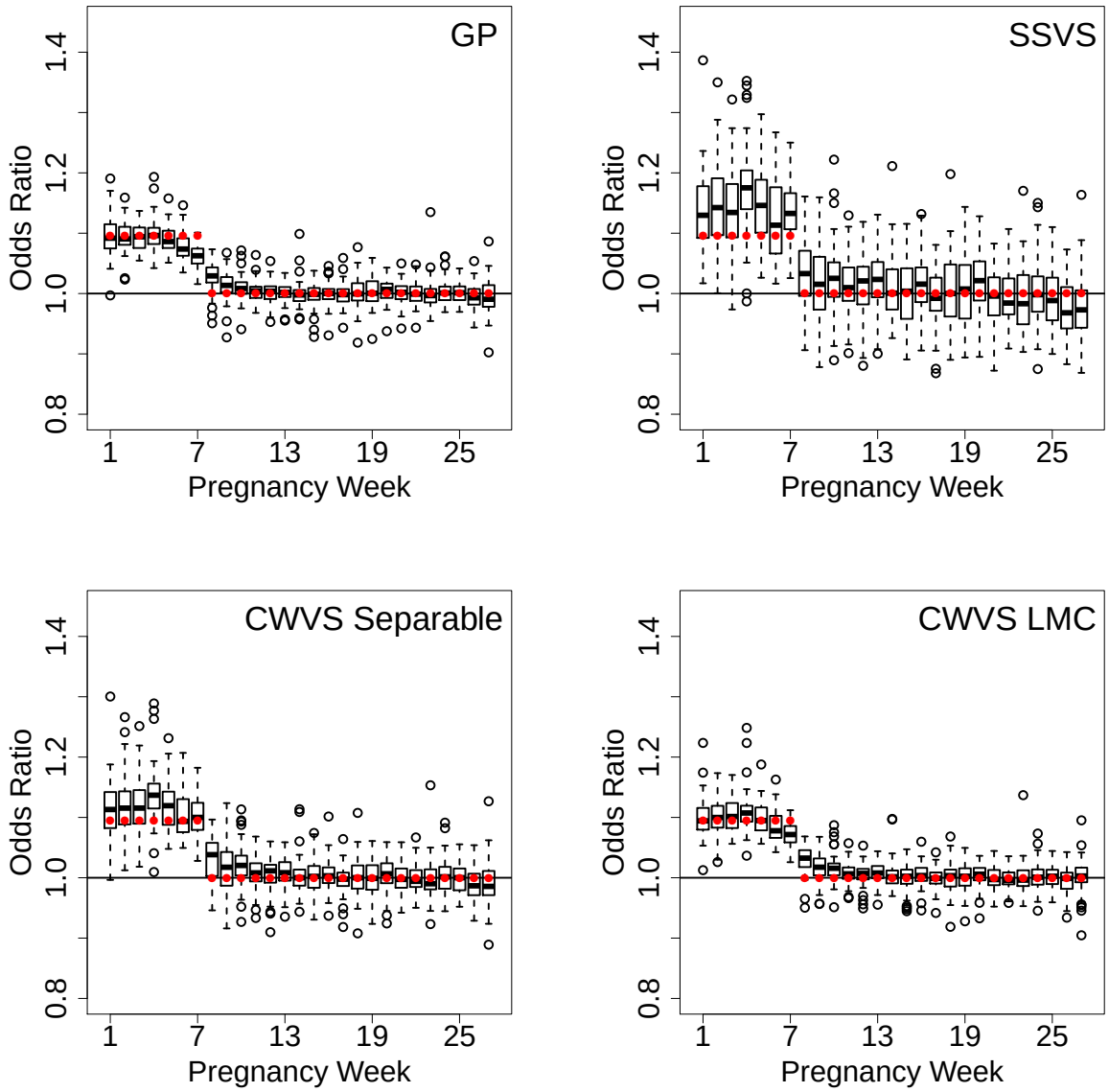

Figure S11: Simulation study results for Setting E7 (mean behavior). Boxplots of the 50 posterior means of $\exp\{\alpha(t)\,|\gamma(t)=1\}$ (just $\exp\{\alpha(t)\}$ for GP) are presented in black. Red dots indicate the true risk parameters. All values presented on the odds ratio scale.

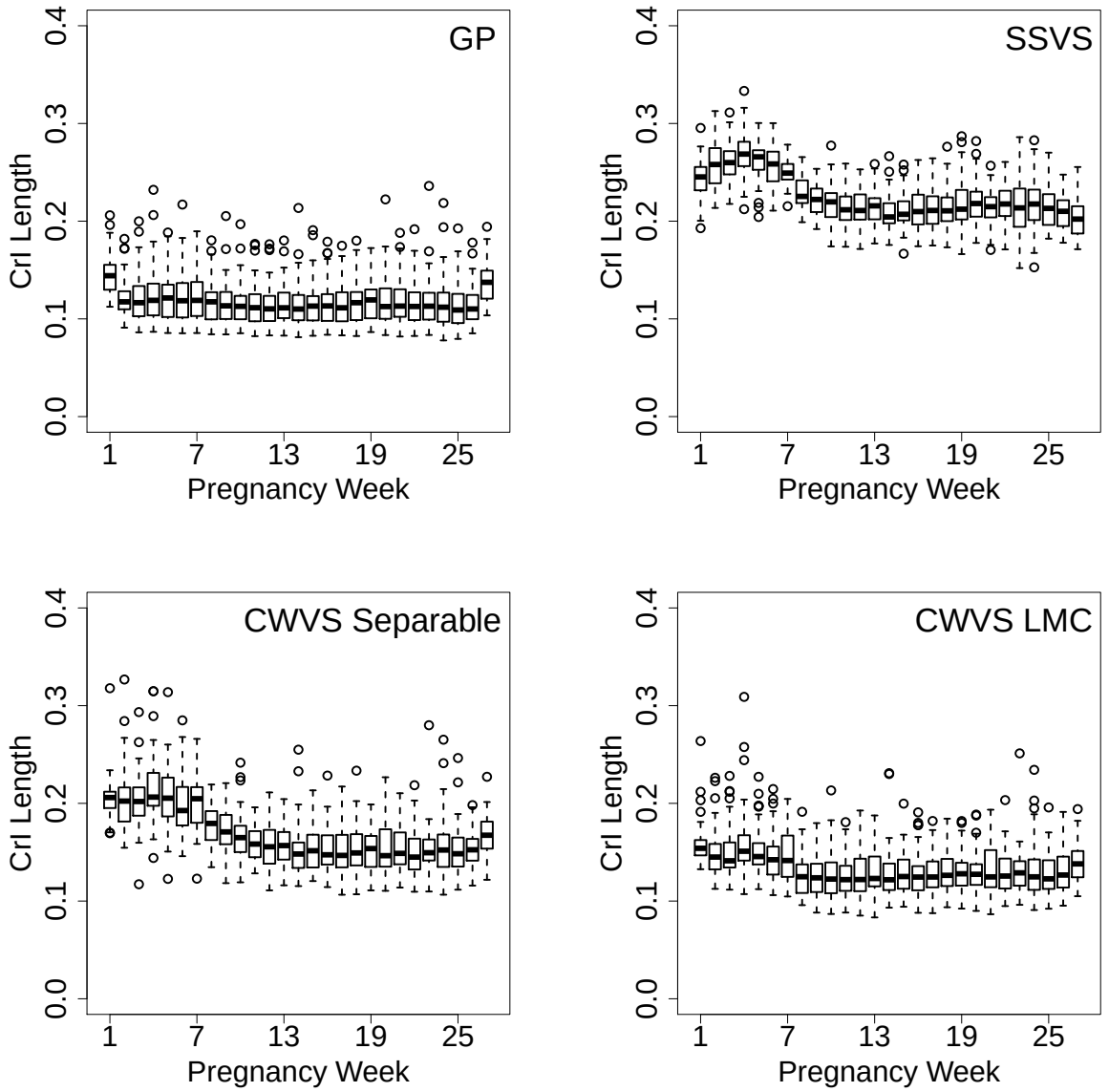

Figure S12: Simulation study results for Setting E7 (uncertainty behavior). Boxplots of the 50 quantile-based 95% credible interval lengths for $\exp\{\alpha(t)\,|\,\gamma(t)=1\}$ (just $\exp\{\alpha(t)\}$ for GP) are presented.

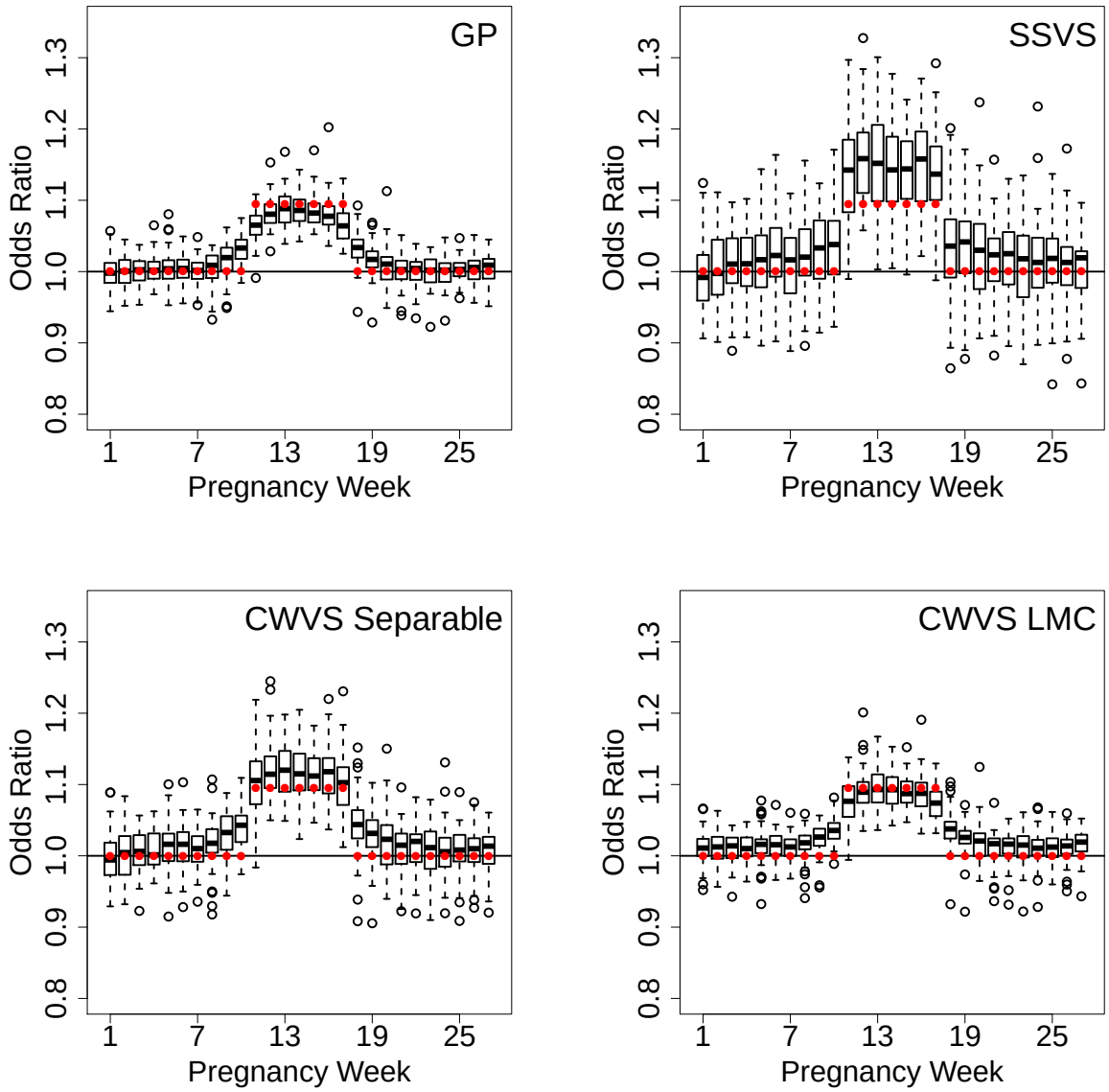

Figure S13: Simulation study results for Setting M7 (mean behavior). Boxplots of the 50 posterior means of $\exp\{\alpha(t)|\gamma(t)=1\}$ (just $\exp\{\alpha(t)\}$ for GP) are presented in black. Red dots indicate the true risk parameters. All values presented on the odds ratio scale.

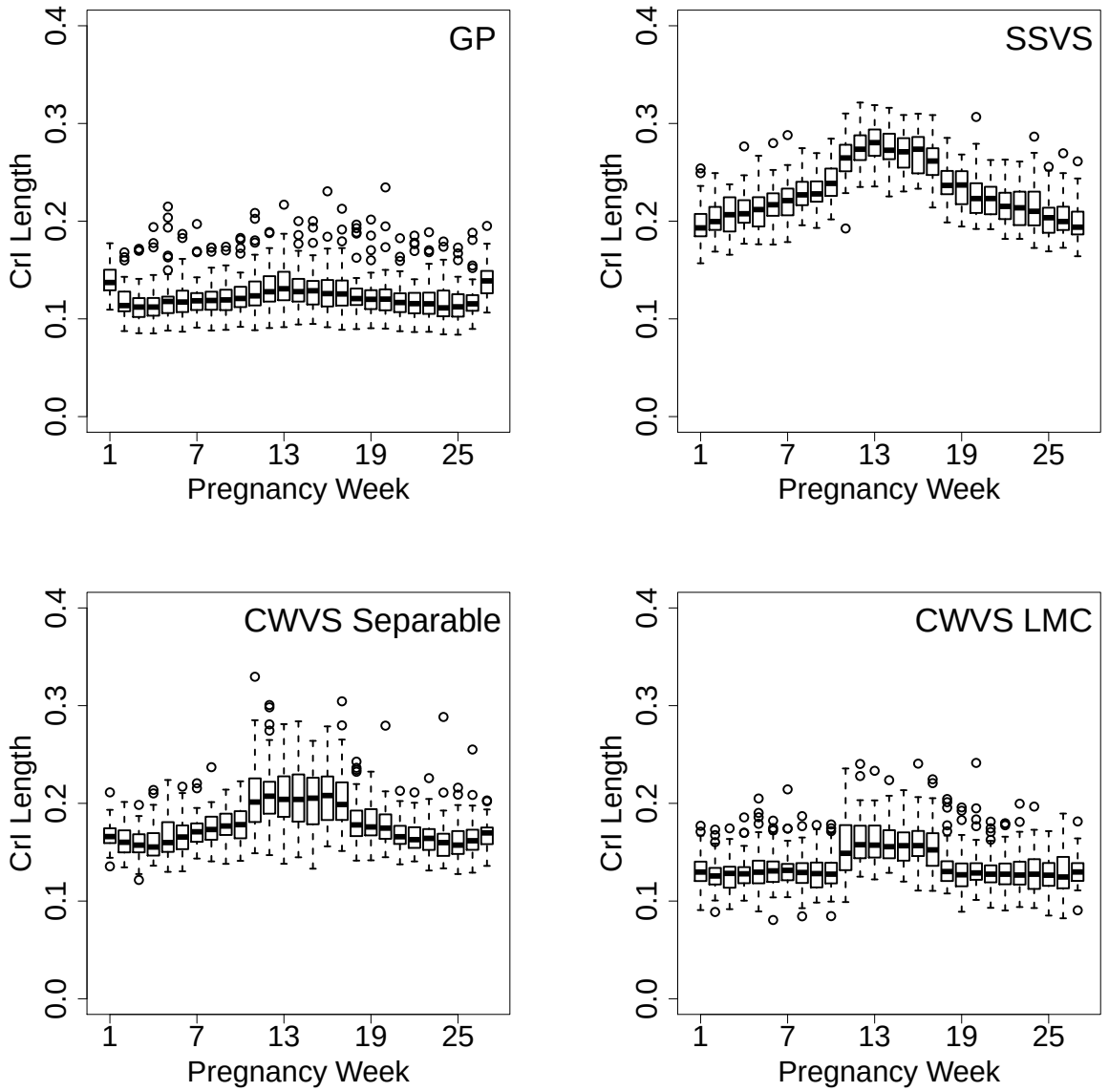

Figure S14: Simulation study results for Setting M7 (uncertainty behavior). Boxplots of the 50 quantile-based 95% credible interval lengths for $\exp\{\alpha(t)\,|\gamma(t)=1\}$ (just $\exp\{\alpha(t)\}$ for GP) are presented.

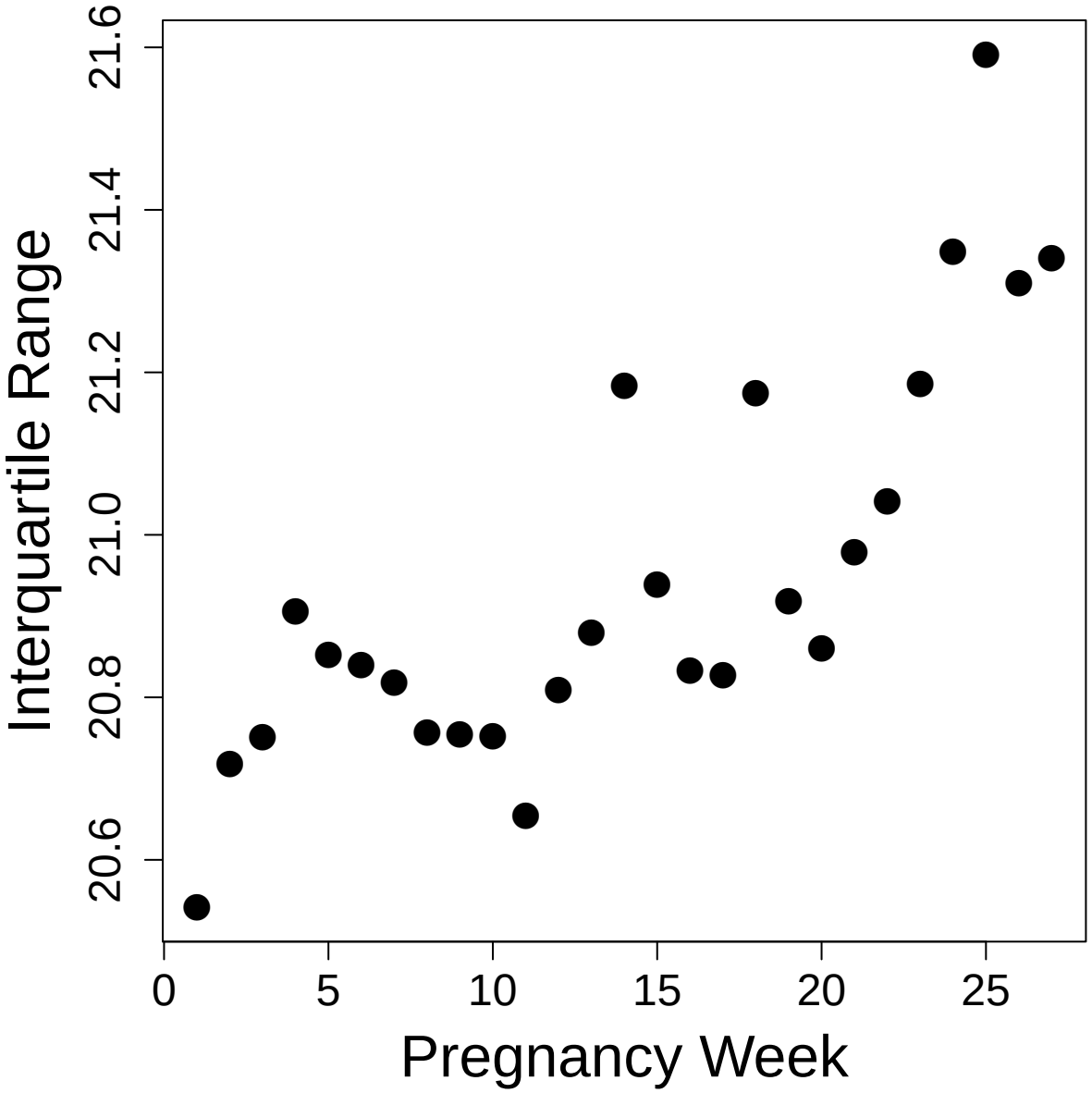

Figure S15: Interquartile range for ozone exposures across pregnancy week.

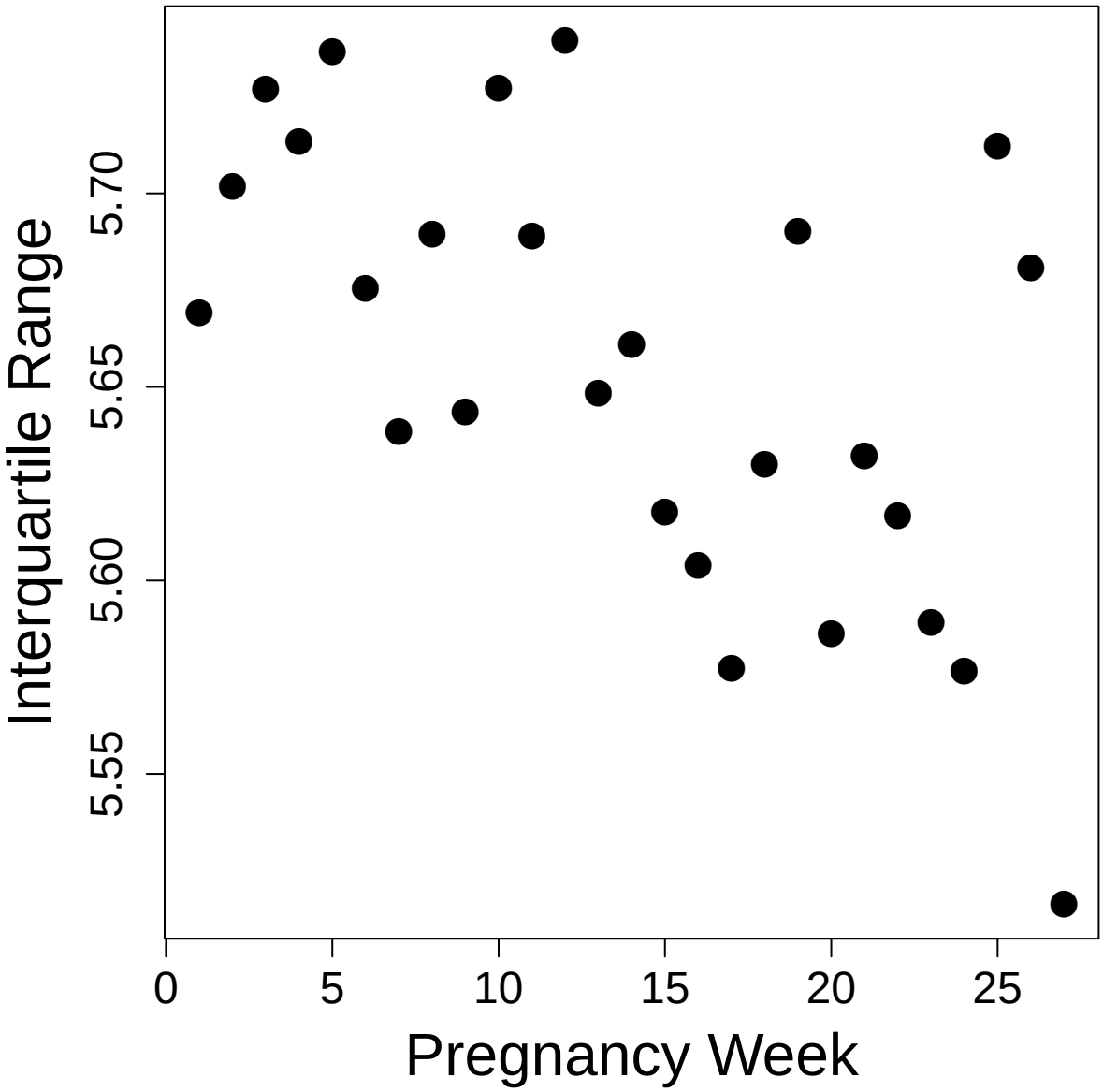

Figure S16: Interquartile range for particulate matter less than 2.5 micrometers in aerodynamic diameter exposures across pregnancy week.

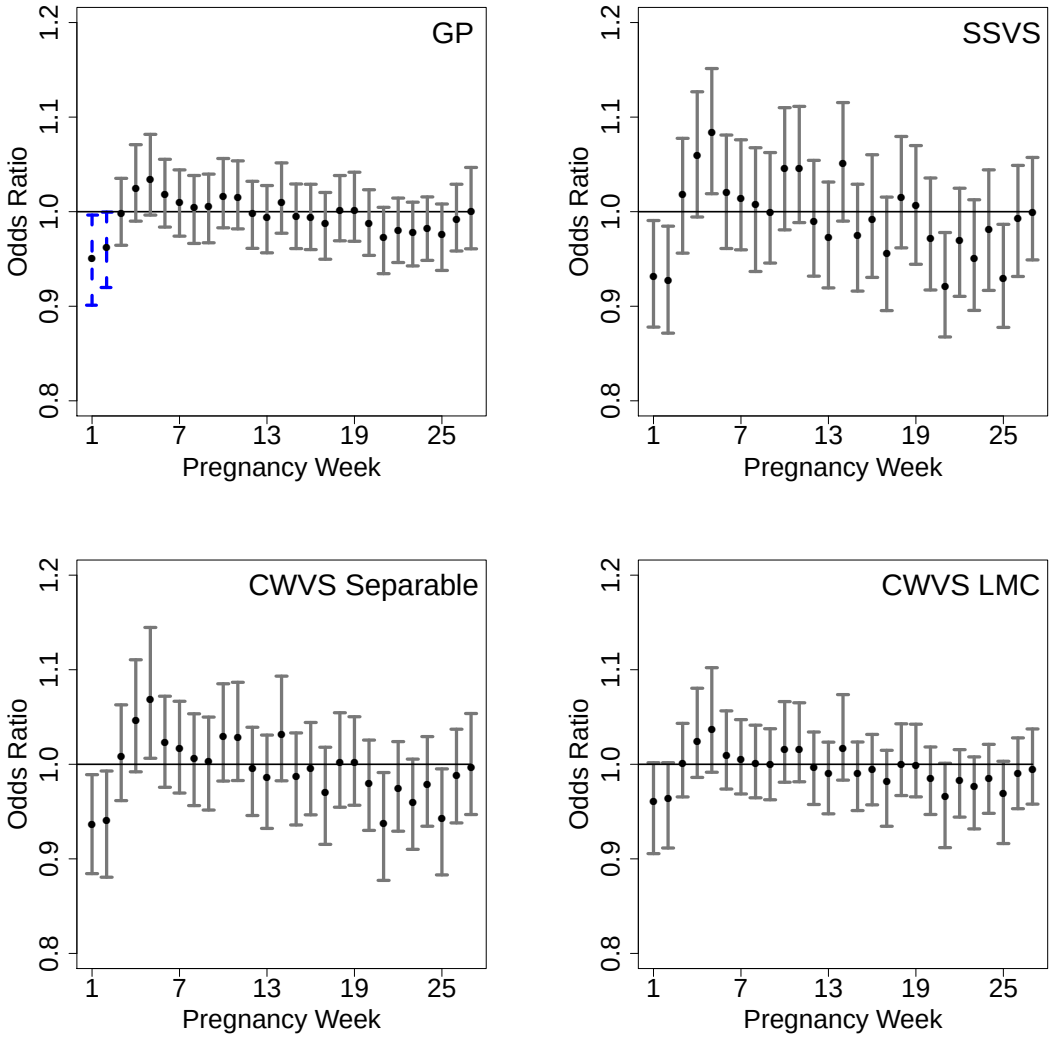

Figure S17: Posterior mean and 95% credible interval results from the very preterm birth and particulate matter less than 2.5 micrometers in aerodynamic diameter (24 hour average) exposure analysis in North Carolina, 2005-2008. Results based on an interquartile range increase in weekly exposure. Weeks identified as part of the critical window set are shown in red/dashed (harmful) and blue/dashed (protective). These definitions depend partly on the posterior inclusion probabilities in Figure S18 for the variable selection methods.

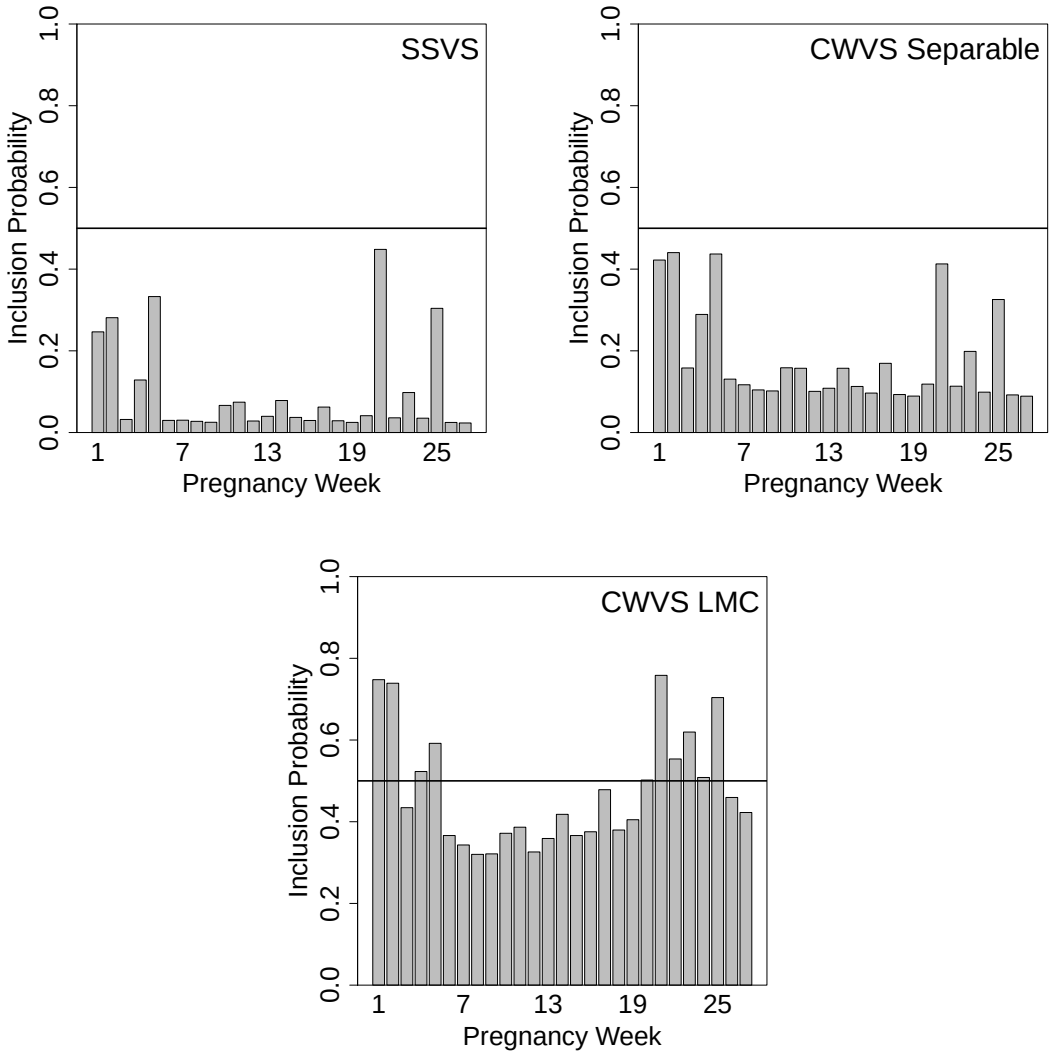

Figure S18: Posterior inclusion probability results from the very preterm birth and particulate matter less than 2.5 micrometers in aerodynamic diameter (24 hour average) exposure analysis in North Carolina, 2005-2008.

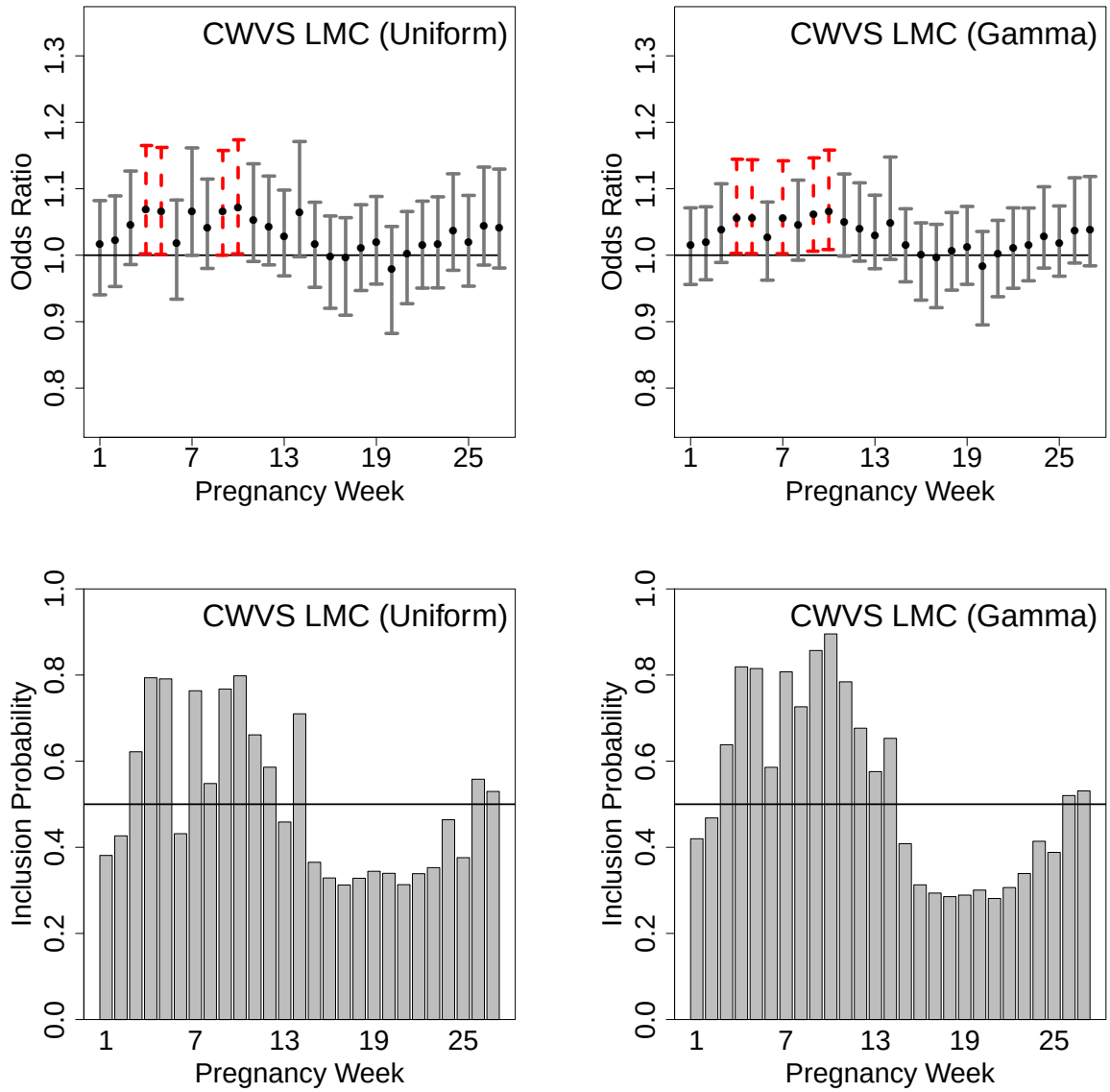

Figure S19: Sensitivity analysis results from the very preterm birth and ozone (8 hour maximum) exposure analysis in North Carolina, 2005-2008. Uniform: $\phi_j \overset{\text{iid}}{\sim} \text{Uniform}\,(0.00, 9.21)$; Gamma: $\phi_j \overset{\text{iid}}{\sim} \text{Gamma}\,(1.00, 1.00)$; $j = 1, 2$.

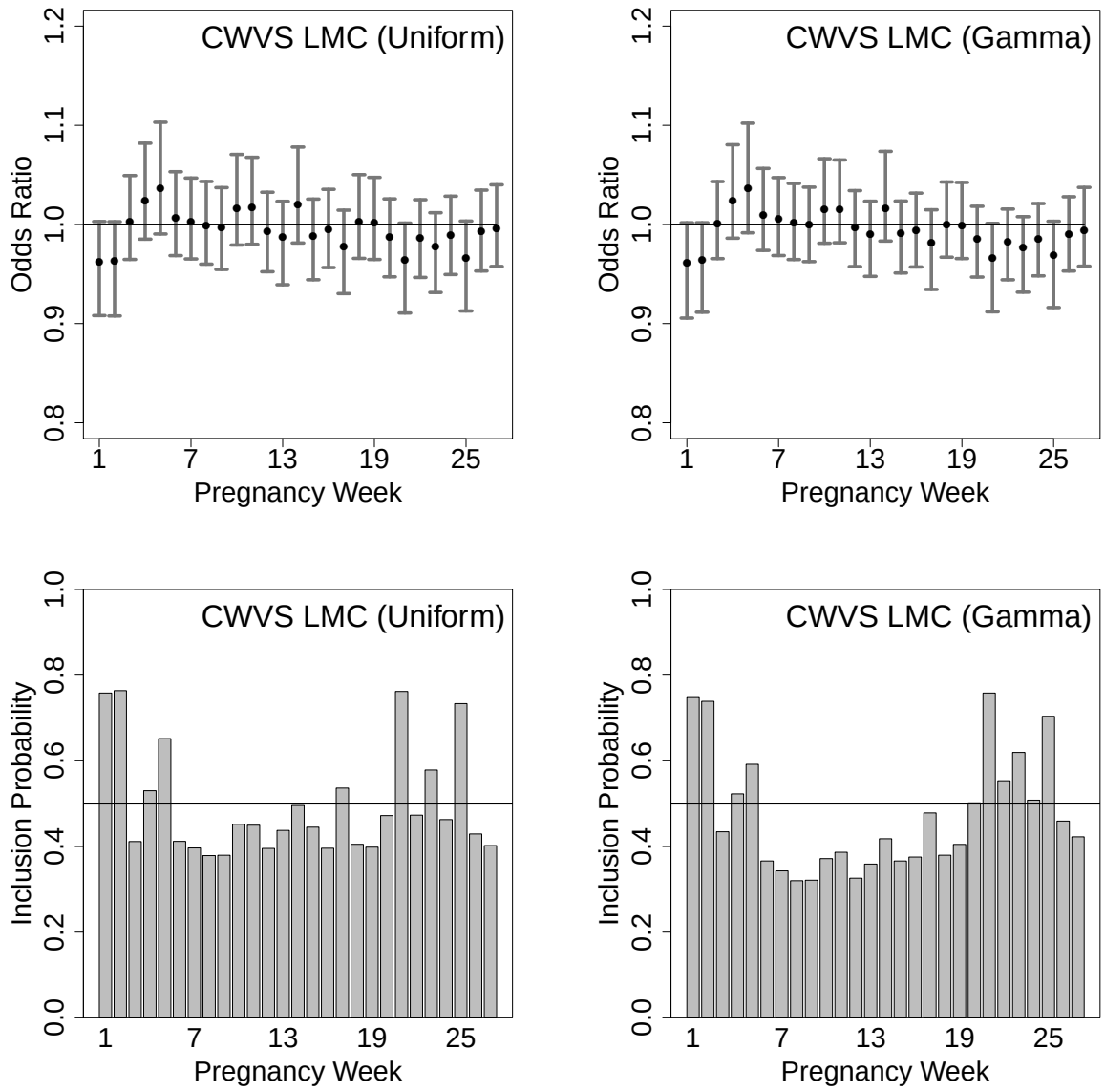

Figure S20: Sensitivity analysis results from the very preterm birth and particulate matter less than 2.5 micrometers in aerodynamic diameter (24 hour average) exposure analysis in North Carolina, 2005-2008. Uniform: $\phi_j \overset{\text{iid}}{\sim} \text{Uniform}\,(0.00, 9.21)$; Gamma: $\phi_j \overset{\text{iid}}{\sim} \text{Gamma}\,(1.00, 1.00)$; $j = 1, 2$.

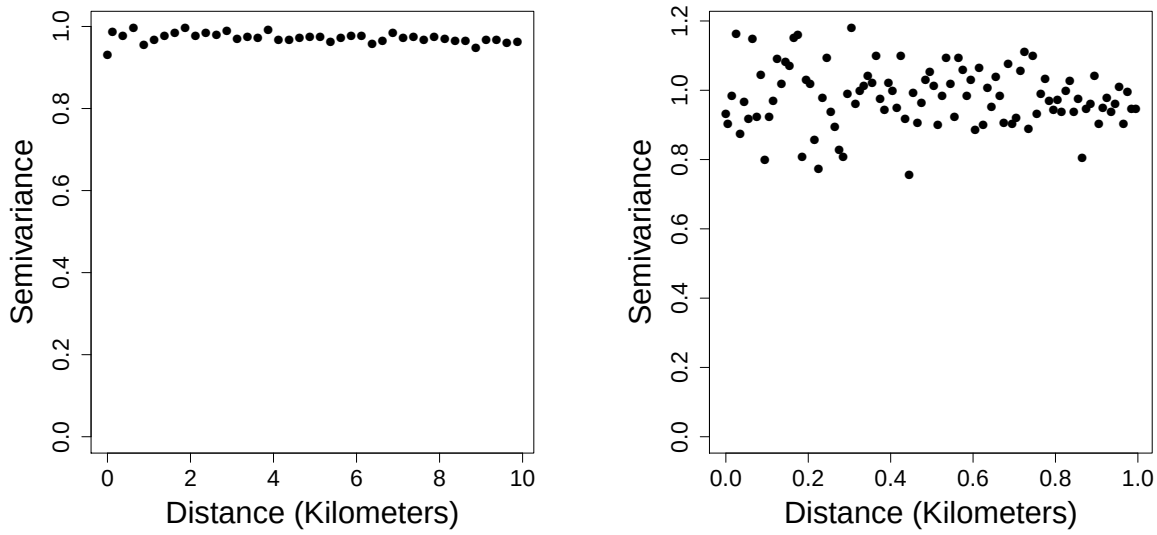

Figure S21: Empirical semivariogram estimates at different distances based on Pearson residuals obtained from the traditional first and second trimester averages model fit from the very preterm birth and ozone (8 hour maximum) exposure analysis in North Carolina, 2005-2008.

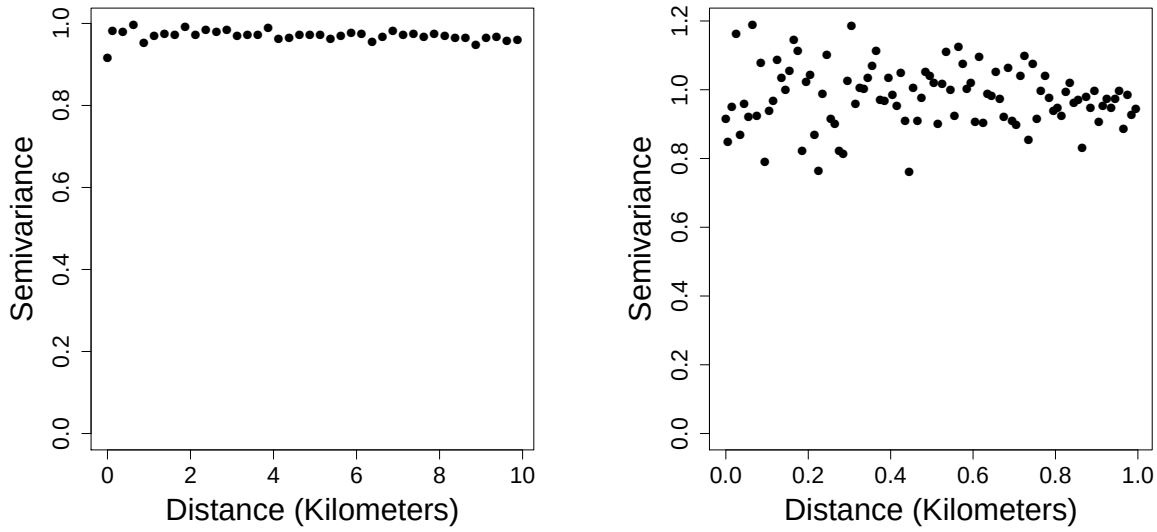

Figure S22: Empirical semivariogram estimates at different distances based on Pearson residuals obtained from the traditional first and second trimester averages model fit from the very preterm birth and particulate matter less than 2.5 micrometers in aerodynamic diameter (24 hour average) exposure analysis in North Carolina, 2005-2008.

References

Gelfand, Alan E and Smith, Adrian FM. (1990). Sampling-based approaches to calculating marginal densities. *Journal of the American Statistical Association* **85**(410), 398–409.

Geman, Stuart and Geman, Donald. (1984). Stochastic relaxation, Gibbs distributions, and the Bayesian restoration of images. *IEEE Transactions on Pattern Analysis and Machine Intelligence* **PAM1-6**(6), 721–741.

Metropolis, Nicholas, Rosenbluth, Arianna W, Rosenbluth, Marshall N, Teller, Augusta H and Teller, Edward. (1953). Equation of state calculations by fast computing machines. *The Journal of Chemical Physics* **21**(6), 1087–1092.

Polson, Nicholas G, Scott, James G and Windle, Jesse. (2013*a*). Bayesian inference for logistic models using Pólya–Gamma latent variables. *Journal of the American statistical Association* **108**(504), 1339–1349.

Polson, Nicholas G., Scott, James G. and Windle, Jesse. (2013*b*). Bayesian inference for logistic models using Pólya-Gamma latent variables. Most recent version: Feb. 2013.

R Core Team. (2017). *R: A Language and Environment for Statistical Computing*. R Foundation for Statistical Computing, Vienna, Austria.